Molecular Therapy
Nucleic Acids
Original Article

An mRNA vaccine induces antimycobacterial immunity by activating DNA damage repair and autophagy

Dan Chen,[1,10] Weili Huang,[1,10] Lifang Shen,[2] Junli Zhang,[2] Zhifen Pan,[3] Chen Zhang,[1] Yuting Tang,[1] Ziwei Zhou,[1] Jie Tao,[4] Geyang Luo,[4] Shifeng Zhang,[1] Jing Zhou,[4] Shuqin Xu,[2] Meng Zhang,[1] Yeyu Li,[1] Yi Fang,[5] Fanfan Zhao,[5] Lei Huang,[5] Hangwen Li,[5] Hua Yang,[6] Hong Lv,[2,7] Wei Sha,[6] Bo Yan,[4] Jun Liu,[8] and Lu Zhang[1,7,9]

[1]Department of Microbiology, School of Life Sciences, Fudan University, Shanghai 200438, China; [2]State Key Laboratory of Genetic Engineering, Department of Genetics, School of Life Science, Fudan University, Shanghai 200438, China; [3]Department of Respiratory Medicine, The First Hospital of Jiaxing in Zhejiang Province, Affiliated Hospital of Jiaxing University, Jiaxing 314000, China; [4]Center for Tuberculosis Research, Shanghai Public Health Clinical Center, Fudan University, Shanghai 201508, China; [5]Stemirna Therapeutics, Shanghai 201206, China; [6]Clinic and Research Centre of Tuberculosis, Shanghai Key Laboratory of Tuberculosis, Shanghai Pulmonary Hospital, Tongji University, Shanghai 200400, China; [7]Shanghai Engineering Research Center of Industrial Microorganisms, Shanghai 200438, China; [8]Department of Molecular Genetics, University of Toronto, Toronto, ON M5S 1A8, Canada; [9]MOE Engineering Research Center of Gene Technology, Shanghai 200438, China

Effective vaccines are urgently needed for the control of tuberculosis (TB). Here, we report that an mRNA TB vaccine is highly effective and exhibits both prophylactic and therapeutic activity in the zebrafish model of TB. Adult zebrafish immunized with the mRNA vaccine survived significantly longer after *Mycobacterium marinum* challenge compared to those immunized with the DNA vaccine. Furthermore, post-infection treatment with the mRNA vaccine drastically reduced the bacterial burden. The mRNA vaccine activated multiple DNA break repair systems that are essential for the normal development and function of adaptive immunity, but did not activate the canonical DNA damage responses that promote cell death. This highlights a profound connection between DNA damage repair and the activation of immune responses under physiological processes of immunization. Remarkably, the mRNA vaccine induced autophagy in granulomas, coinciding with bacterial killing and cell survival. Collectively, these findings demonstrate that the mRNA vaccine elicits potent innate and adaptive immunity, providing effective host protection against mycobacterial challenge.

INTRODUCTION

Tuberculosis (TB), caused by *Mycobacterium tuberculosis* (*M. tb*), is the leading cause of death from a single infectious agent, which caused 1.3 million deaths and 7.5 million newly diagnosed cases in 2022. An estimated 2 billion people are latently infected with *M. tb*, which is called latent TB infection (LTBI).[1] Notably, TB mortality increased during the COVID-19 pandemic for the first time in a decade.[2] Bacille Calmette-Guérin (BCG), a live attenuated strain of *M. bovis*, is the only approved TB vaccine. BCG has been used clinically since the 1920s, with over 4 billion doses administered. While providing over 80% protection against disseminated TB in children,[3,4] BCG is limited in its ability to protect adolescents and adults from developing transmittable pulmonary TB, with efficacy rates varying widely from 0% to 80%.[5,6] Another problem is that BCG does not prevent the reactivation of LTBI, complicating efforts to control the disease. This challenge is compounded by the lack of antibiotics capable of fully eradicating latent TB. The global burden of TB, combined with the increasing prevalence of drug-resistant *M. tb* strains (both multidrug- and extensively drug-resistant TB), emphasizes the importance of developing effective TB vaccines to achieve the World Health Organization's goal of ending the TB epidemic by 2035.

Despite extensive efforts in the past 30 years, a new vaccine offering better protection than BCG has yet to be developed. Current vaccine candidates in clinical trials development fall into two categories: (1) whole cell-derived (attenuated *M. tb* and recombinant BCG) and (2) subunit (adjuvanted protein and viral vectored DNA) vaccines.[7] Most subunit vaccines consist of selected *M. tb* antigens that are expressed in replication-deficient viral vectors or are administered as purified protein/adjuvant combination. As a prophylactic vaccine, none of these subunit vaccines has proven to be superior to BCG in animal models. As such, subunit vaccines are being evaluated for the prevention of disease in *M. tb*-infected individuals. While a recent clinical study showing 49.7% efficacy of the subunit vaccine M72/AS01$_E$ is

Received 17 July 2024; accepted 22 November 2024;
https://doi.org/10.1016/j.omtn.2024.102402.

[10]These authors contributed equally

Correspondence: Bo Yan, Center for Tuberculosis Research, Shanghai Public Health Clinical Center, Fudan University, Shanghai 201508, China.
E-mail: bo.yan@shphc.org.cn
Correspondence: Jun Liu, Department of Molecular Genetics, University of Toronto, Toronto, ON M5S 1A8, Canada.
E-mail: jun.liu@utoronto.ca
Correspondence: Lu Zhang, Department of Microbiology, School of Life Sciences, Fudan University, Shanghai 200438, China.
E-mail: zhanglu407@fudan.edu.cn

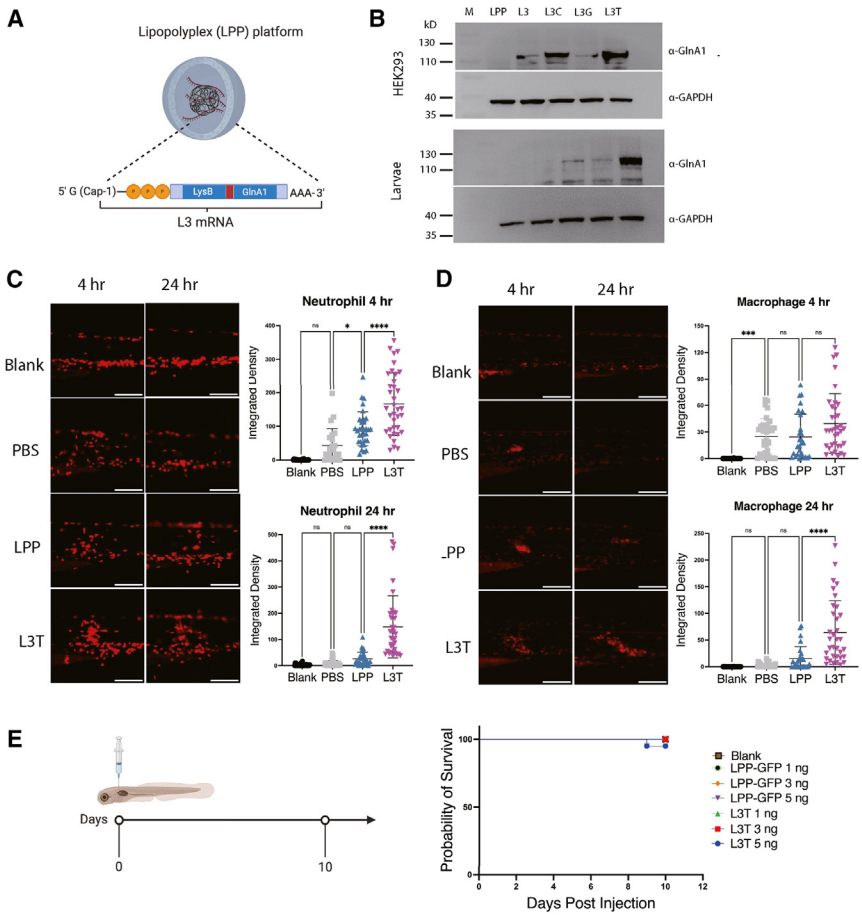

Figure 1. Construction and characterization of L3T mRNA vaccine

(A) Scheme of the LPP-L3 mRNA design. (B) L3 protein expression *in vitro* (HEK293T cells) and *in vivo* (zebrafish larvae) at 24 hpost-transfection or post-injection of mRNA. (C and D) Neutrophil and macrophage recruitment at 4 and 24 h post-injection of 3 ng L3T mRNA ($n \geq 30$). Blank: larvae without injection. PBS, LPP: larvae injected with PBS or LPP-GFP. Statistical analysis was performed using one-way ANOVA. $^{*}p < 0.05$; $^{***}p < 0.001$; $^{****}p < 0.0001$. (E) L3T mRNA safety profile in larvae ($n = 20$). Blank: larvae without injection.

encouraging,[8] there is room for improvement. Multiple approaches have been employed to develop new live vaccines, including various recombinant BCGs and attenuated *M. tb* strains.[9] Of these, only a few have outperformed BCG in animal models.[10–12] Although these live vaccine candidates offer better protection and have the potential to replace BCG, they are unlikely to be effective against LTBI.

The extraordinary success of mRNA COVID-19 vaccines has rekindled significant interest in using mRNA for delivering vaccines or therapeutic proteins for other diseases.[13,14] Since mRNA does not integrate into the genome, it mitigates concerns about genotoxicity and broadens accessibility to immunocompromised individuals.[15] In addition, a single mRNA can encode multiple antigens, strengthening the immune response.[15] However, there is a scarcity of publications on mRNA vaccines targeting TB.[16,17] We constructed an mRNA TB vaccine delivered by lipid nanoparticles and tested its activity in the zebrafish model of TB. Zebrafish is a natural host of *M. marinum*, a close relative of the *M. tb* complex. Infection of zebrafish with *M. marinum* recapitulates many aspects of human TB and has proven to be a useful model in studying innate immunity, TB granulomas, and host-pathogen interactions.[18] Here, we report that the mRNA TB vaccine exhibits superior prophylactic activity in adult zebrafish against *M. marinum* infection. Remarkably, it also demonstrates highly potent post-infection therapeutic activity. The mRNA vaccine activates DNA damage repair systems essential for the development of adaptive immunity, as well as autophagy, a key player in innate immunity. Collectively, our study has provided new insights into the immune mechanisms required for the control of mycobacterial infection and demonstrated the promising potential of the mRNA platform for TB vaccine development.

RESULTS

An mRNA vaccine L3T increases the recruitment of innate immune cells

Glutamine synthetase (GlnA1) is an essential enzyme of *M. tb* and plays a role in virulence.[19] *M. tb* secretes high levels of GlnA1 into the culture media, making it a good candidate for vaccine development.[20] Lysin B (LysB) is a lytic enzyme of mycobacteriophages that can inhibit the growth of multiple mycobacterial species, including *M. tb* and *M. marinum*.[21] We reasoned that a fusion protein (L3) combining GlnA1 and LysB could be used to construct prophylactic and therapeutic vaccines. To do this, mRNA sequences encoding LysB, GlnA1, and a 9-amino acid linker between them were designed and produced. Codon optimization using different algorithms generated three mRNA sequences, denoted as L3T, L3C, and L3G. Additional modifications were made to increase the mRNA stability and expression in host cells. The final mRNA sequences contain a 5′ Cap-1, a 5′ highly stable UTR from the β-globin gene of *Xenopus laevis*[22]; an optimized coding sequence of L3, a 3′ UTR of α-globin from humans[23]; and a poly(A) tail (Figure 1A). In addition, uridine was substituted with 1-methylpseudouridine (m1Ψ) to decrease immunogenicity of the RNA,[24] the same modification used in the mRNA COVID-19 vaccines.[25] A lipopolyplex (LPP) platform was used to deliver the mRNA antigen, in which the negatively charged mRNA molecules were packaged with a cationic poly-(β-amino ester) polymer and then encapsulated in a phospholipid bilayer shell (Figure 1A).[26]

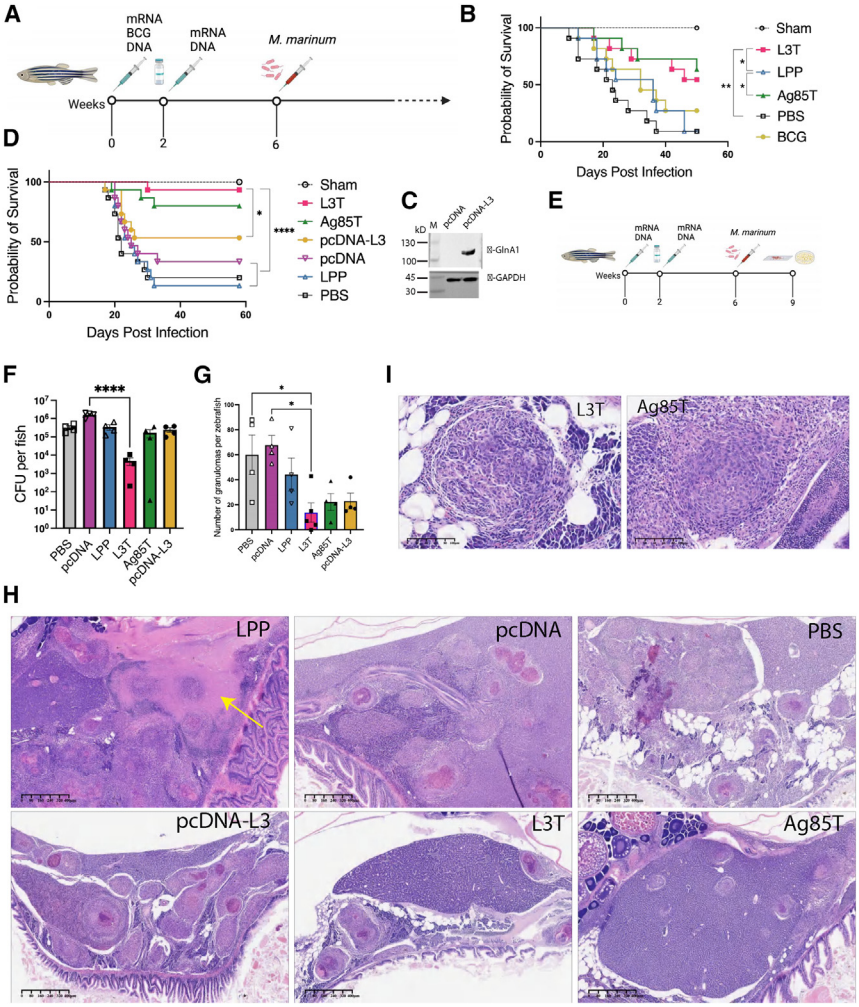

Figure 2. L3T mRNA vaccine protects zebrafish against *M. marinum* infection

(A and E) Schemes of vaccine immunization and *M. marinum* infection. (B and D) Survival curves of adult zebrafish (n = 11–15) injected i.m. with mRNA or DNA twice with a 2-week interval, or BCG one time, followed by intraperitoneal injection of 500 CFU of *M. marinum* 535. Zebrafish injected with PBS or LPP or pcDNA were used as negative controls. Statistical analysis was performed using the log rank (Mantel-Cox) test. $^{*}p < 0.05$; $^{**}p < 0.01$; $^{****}p < 0.0001$. (C) pcDNA-L3 expression in HEK293 T cells at 24 h transfection. (F and G) Bacterial burden (F) or number of granulomas (G) in zebrafish 3 weeks after *M. marinum* infection (n = 4 or 5). One-way ANOVA was performed for statistical analysis. $^{*}p < 0.05$; $^{****}p < 0.0001$. (H and I) Representative H&E staining of zebrafish tissues 3 weeks after *M. marinum* infection. Arrow in (H) indicates the caseous granulomas.

To examine the expression of the L3 mRNA, HEK293T cells were transfected with the three L3 mRNAs, and the cell lysates were analyzed by western blot. The results showed that both L3T and L3C were expressed at high levels, with L3T showing higher expression levels than L3C in zebrafish larvae (Figure 1B). Therefore, L3T was selected for subsequent studies.

Successful vaccination begins with local activation of the innate immune system. After intramuscular (i.m.) injection, proinflammatory cytokines and chemokines generated by the local resident cells recruit the innate immune cells, including macrophages, neutrophils, and dendritic cells, to the injection site. Antigens are taken up and transported to the draining lymph lode to activate the adaptive immune response.[27] Previously, it was reported that the LPP nanoparticles facilitated the uptake of the encapsulated mRNA by dendritic cells.[26] To investigate whether L3T can effectively attract innate immune cells to the injection site, we used transgenic zebrafish larvae from the Tg(*mpeg1::LRLG*) and Tg(*lyz::DsRed*) lines, where macrophages and neutrophils express red fluorescence protein and DsRed, respectively. These larvae were injected with wither L3T or a control (LPP-GFP) containing encapsulated GFP mRNA. We observed increased recruitment of both neutrophils and macrophages at the L3T injection site 4- h post-injection, with the neutrophil recruitment being more pronounced (Figures 1C and 1D). The L3T-mediated immune cell recruitment lasted for at least 24 h post-injection, at which point the experiment was terminated. The dose (3 ng per larva) of L3T used in this experiment was based on its safety profile, as all larvae (n = 20) injected with this dose of L3T survived for 10 days (Figure 1E).

L3T mRNA vaccine protects zebrafish against *M. marinum* infection

To examine the protective efficacy of L3T, adult zebrafish were immunized twice (at 2-week intervals) with L3T or the negative control LPP. Ag85A is a commonly used antigen for the construction of subunit TB vaccines.[7] As a positive control and also for comparison, LPP-Ag85A mRNA was included in this experiment. The Ag85A mRNA, referred to as Ag85T, was optimized and modified in a manner similar to the L3T mRNA. Zebrafish immunized once with BCG was also included for comparison. Four weeks after the final vaccination, zebrafish were challenged with *M. marinum* 535, and their survival was monitored (Figure 2A).

The survival curves were plotted using the Kaplan-Meier method. Log rank analysis revealed that zebrafish immunized with the mRNA vaccine L3T or Ag85T survived significantly longer than the negative control groups (LPP or PBS) (Figure 2B). The mRNA vaccines also appeared to perform better than BCG, with the difference approaching statistical significance (p = 0.08).

We repeated this experiment and included an L3 DNA vaccine (pcDNA-L3) for comparison. We cloned the coding sequence of L3 into the pcDNA3.1+ expression vector and confirmed its expression in HEK293T cells (Figure 2C). The DNA vaccine was administered twice, with a 2-week interval, but at a much higher dose than the mRNA vaccines (6 vs. 1 μg per fish) (Figure 2A). Consistent with the previous experiment, the L3T-immunized zebrafish survived significantly longer than the negative control groups (PBS, LPP, and pcDNA), and nearly all fish (14 out of 15) in the L3T group remained alive at 60 days post-infection (dpi; Figure 2D). Notably, while encoding the same L3 protein antigen, the L3T mRNA performed significantly better than its DNA counterpart (pcDNA-L3), despite being administered at a lower dose. Zebrafish vaccinated with Ag85T again survived significantly longer than the negative control groups ($p = 0.0001$), but its survival curve was not statistically different from that of the pcDNA-L3 group.

In parallel with the long-term survival experiment (Figure 2D), we set up another short-term experiment in which the zebrafish were sacrificed at 3 weeks post-*M. marinum* infection and then subjected to bacterial burden and histology analysis (Figure 2E). The bacterial burden in zebrafish at 3 weeks post-infection is in accordance with the survival curve analysis. Zebrafish immunized with L3T had an ∼2 $\log_{10}$ lower bacterial number than the other groups (Figure 2F).

Granulomas are a hallmark of TB pathology, representing both the acquisition of an infection and the induction of the host immune response.[28] While granulomas benefit the host by constraining the pathogen, they also serve as a niche for bacterial dissemination.[29] The outcome depends on the interplay between bacterial virulence and host immunity. In zebrafish without immunization (the negative control groups PBS, LPP, and pcDNA), numerous granulomas were detected in multiple organs, including the liver, kidneys, spleen, intestines, and testis. These granulomas were heterogeneous in size, the appearance of necrotic centers, and the level of necrosis (Figure 2H). Notably, many of these granulomas appeared as clusters, indicating extensive bacterial dissemination in the same region, with new granulomas emerging as the bacteria spreads to adjacent areas. Fewer numbers of granulomas were detected in the L3T group, with the majority (4/5) of fish having <20 granulomas. In comparison, the control groups had between 20 and 90 granulomas (Figure 2G). A large number of bacteria were detected in necrotizing granulomas, especially those that have caseous necrosis. Thus, the number of necrotizing granulomas roughly correlates with the bacterial burden.

Granulomas in the L3T group tended to be isolated rather than clustered, as observed in the other groups (PBS, LPP, pcDNA, and pcDNA-L3) (Figure 2H). Interestingly, some granulomas in the L3T and Ag85T groups appeared to be much healthier; they were non-necrotizing and singly located, thus unlikely to be newly formed due to bacterial spread (Figure 2I). They also contained no detectable bacteria, suggesting that these granulomas may have successfully resolved the infection and were recovering. This type of granuloma was not detected in the control groups.

Collectively, these results demonstrate that mRNA vaccines, especially L3T, exhibit a superior prophylactic activity to BCG or the DNA-based vaccine.

L3T mRNA vaccine exhibits potent therapeutic activity

To determine whether L3T has post-infection activity, zebrafish larvae were infected with *M. marinum* and after a 24-h infection, treated with L3T or the LPP control (Figure 3A). The *M. marinum* strain used in this experiment, *M. marinum* 535:*gfp*, expresses the GFP protein and enables the analysis of bacterial burden by fluorescence intensity. There was a 1.9- and 2.7-fold reduction of bacterial burden in the L3T group compared to the control group at days 2 and 3 post-treatment, respectively, with both differences being statistically significant (Figure 3B). Consistently, in a parallel long-term experiment, the L3T-treated larvae survived significantly longer than the control groups (LPP or PBS) (Figure 3C).

Next, we extended the treatment experiment to adult zebrafish. Adult zebrafish were infected with *M. marinum* 535 and then treated twice with L3T, once on day 14 and again on day 17 post-infection, and their survival was monitored (Figure 3D). The L3T treatment group survived significantly longer than the control groups (LPP or PBS) (Figure 3E). Consistently, the L3T treatment group showed an ∼1 $\log_{10}$ reduction in bacterial burden at 7 days post-treatment (Figure 3F) and significantly fewer granulomas than the control groups (Figure 3G).

We performed three more L3T treatment experiments. Each time, the zebrafish were infected with a different *M. marinum* strain, including *M. marinum* 1218R, a *whiB4* inactivated strain (*whiB4*:Tn) of *M. marinum*1218R that causes persistent infection in zebrafish,[30] and a rifampicin-resistant (Rif^R) strain of *M. marinum* 535. For comparison, one group of zebrafish was treated daily with rifampicin, a first-line antibiotic for TB treatment, for 7 days starting on day 14 post-infection, while another group was treated with a combination of L3T and rifampicin. At day 24 post-infection, the fish were sacrificed, and the bacterial burden was determined.

The L3T treatment groups consistently had an ∼5-fold reduction in bacterial numbers compared to the control groups (PBS, LPP), and these differences were statistically significant (Figures 3H–3J). Remarkably, the bacterial burden in the L3T treatment groups was similar to that of the rifampicin treatment groups (Figures 3H and 3I), even though the L3T treatment was administered only twice, whereas the rifampicin treatment lasted 1 week, indicating the extraordinary bacterial killing capability of L3T. Intriguingly, no additive or synergistic effect was observed between these two treatments (Figures 3H and 3I). Notably, L3T treatment was even effective against the drug-resistant strain of *M. marinum* (Figure 3J).

Together, these results demonstrate the highly potent bactericidal activity of L3T, suggesting that it can be used for post-infection treatment such as the treatment of LTBI.

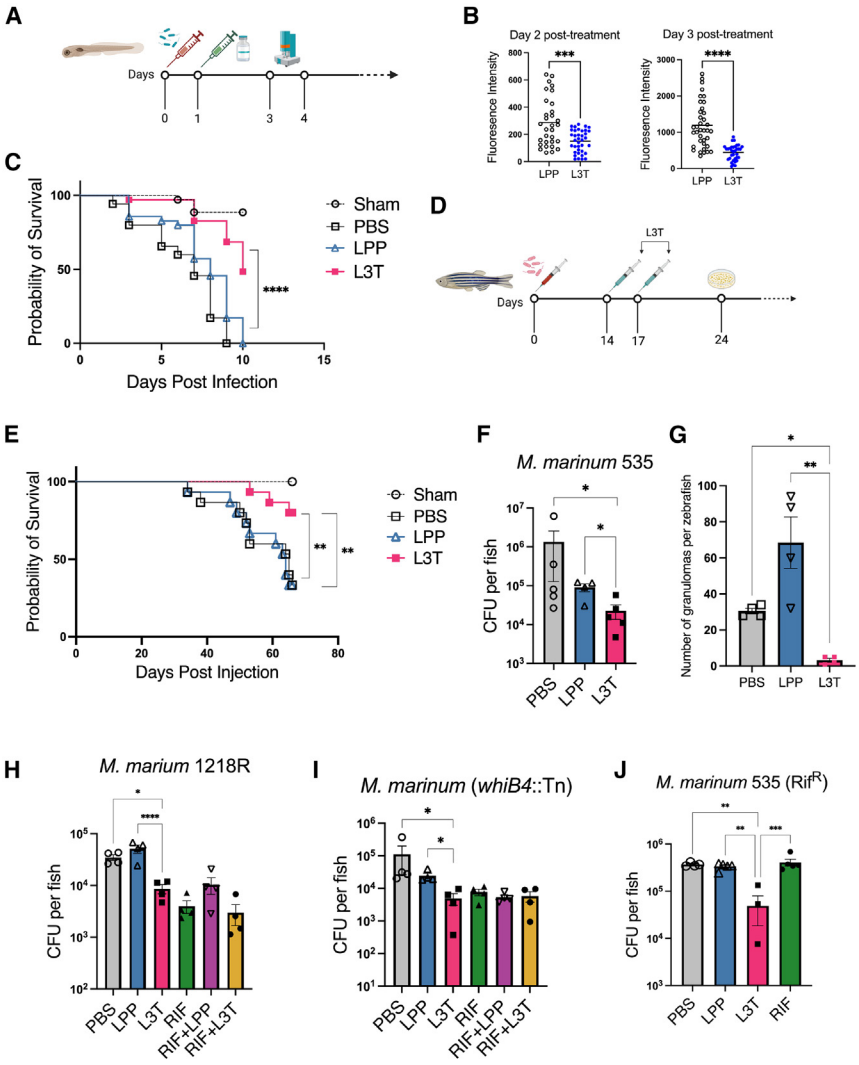

Figure 3. L3T mRNA vaccine exhibits potent therapeutic activity

(A) Scheme of *M. marinum* infection and L3T mRNA treatment in larvae. (B) Bacterial burden was determined at days 2 and 3 post-L3T treatment (n = 35). Mann-Whitney tests were performed for statistical analysis. ***$p < 0.001$; ****$p < 0.0001$. (C) Survival curves of larvae were plotted (n = 35). Log rank test was performed for statistical analysis. ****$p < 0.0001$. (D) Scheme of *M. marinum* infection and L3T mRNA treatment in adult zebrafish. (E) Survival curves of adult zebrafish were plotted (n = 15). Log rank test was performed for statistical analysis. **$p < 0.01$. (F) Bacterial burden of adult zebrafish 1 week after the second L3T treatment (n = 5). (G) Number of granulomas determined by H&E analysis (n = 4). (H–J) Bacterial burden in zebrafish 24 days post-intraperitoneal *M. marinum* infection (n = 4). Zebrafish treated with rifampicin (400 μM, bath treatment, daily for 7 days starting on day 14 post-infection) was used as the positive control. Zebrafish treated with the combination of L3T and rifampicin were also included. One-way ANOVA was performed for statistical analysis. *$p < 0.05$; **$p < 0.01$; ***$p < 0.001$; ****$p < 0.0001$.

L3T mRNA vaccine induces DNA damage repair

Like other teleosts, the zebrafish lack lymph nodes. Instead, the kidney and spleen are the major lymphoid organs of zebrafish and are responsible for the removal of foreign agents and defective blood cells.[31] To understand the immunoprotective mechanisms mediated by the L3T vaccine, we performed RNA sequencing (RNA-seq) analysis of kidneys isolated from zebrafish immunized with the mRNA vaccine and the LPP control. Kidneys from five zebrafish were pooled into one sample, and three pooled samples (a total of 15 kidneys) were collected from each group for RNA-seq analysis.

A total of 302 differentially expressed genes (DEGs) (|log2fold change|>0.58, $q < 0.05$) was detected comprising 111 upregulated and 191 downregulated in the L3T-immunized zebrafish compared to the LPP control group (Figure 4A; Table S1). Gene Ontology (GO) analysis revealed that among the upregulated genes, terms involved in "DNA replication" (q = 2.08E−7) and "cellular response to DNA damage stimulus" (q = 1.3E−3) were significantly enriched (Figure 4B). Many of these genes have function in both DNA damage repair and replication, and thus, they were listed in both categories, including *Dna2*, *Fen1*, *Msh2*, *Mcm9*, *PcnA*, *Pold3*, *Pms2*, *Ssrp1a*, *Spata18*, and *Yars1*.

MSH2 and PMS2 are essential components of the DNA mismatch repair system, which is an evolutionally conserved and post-replicative pathway that contributes to replication fidelity (Figure 4C).[32] MSH2 is involved in the lesion-recognition step. MutSα (MSH2/MSH6 heterodimer) recognizes base mismatch and 1- to 2-nt insertion-deletion loops (IDLs), while MutSβ (MSH2/MSH3 heterodimer) recognizes large IDLs.[32] Next, the MutL complexes, particularly MutLα (MLH1/PMS2 heterodimer), are recruited onto DNA and regulate the termination of mismatch-provoked excision.[32] Following the excision of mismatched nucleotides by EXO1, the replacement DNA is synthesized by DNA polymerase δ. The *Pold3* gene encodes the 66-kDa subunit of DNA polymerase δ and regulates its activity. PCNA plays an important role, not only in the mismatch recognition step but also in the subsequent DNA synthesis (Figure 4C).[32]

MCM9 and DNA2 are involved in double-strand break (DSBs) repair by homologous recombination (HR; Figure 4C). DSBs are detrimental to cells, and unresolved DSBs are implicated in various human disorders and cancers. Organisms have evolved to employ two major pathways—HR and non-homologous end joining—to resolve DSBs.[32] For short-range resection, the MRE11-RAD50-NBS1 (MRN) complex recognizes a DSB and initiates resection to promote

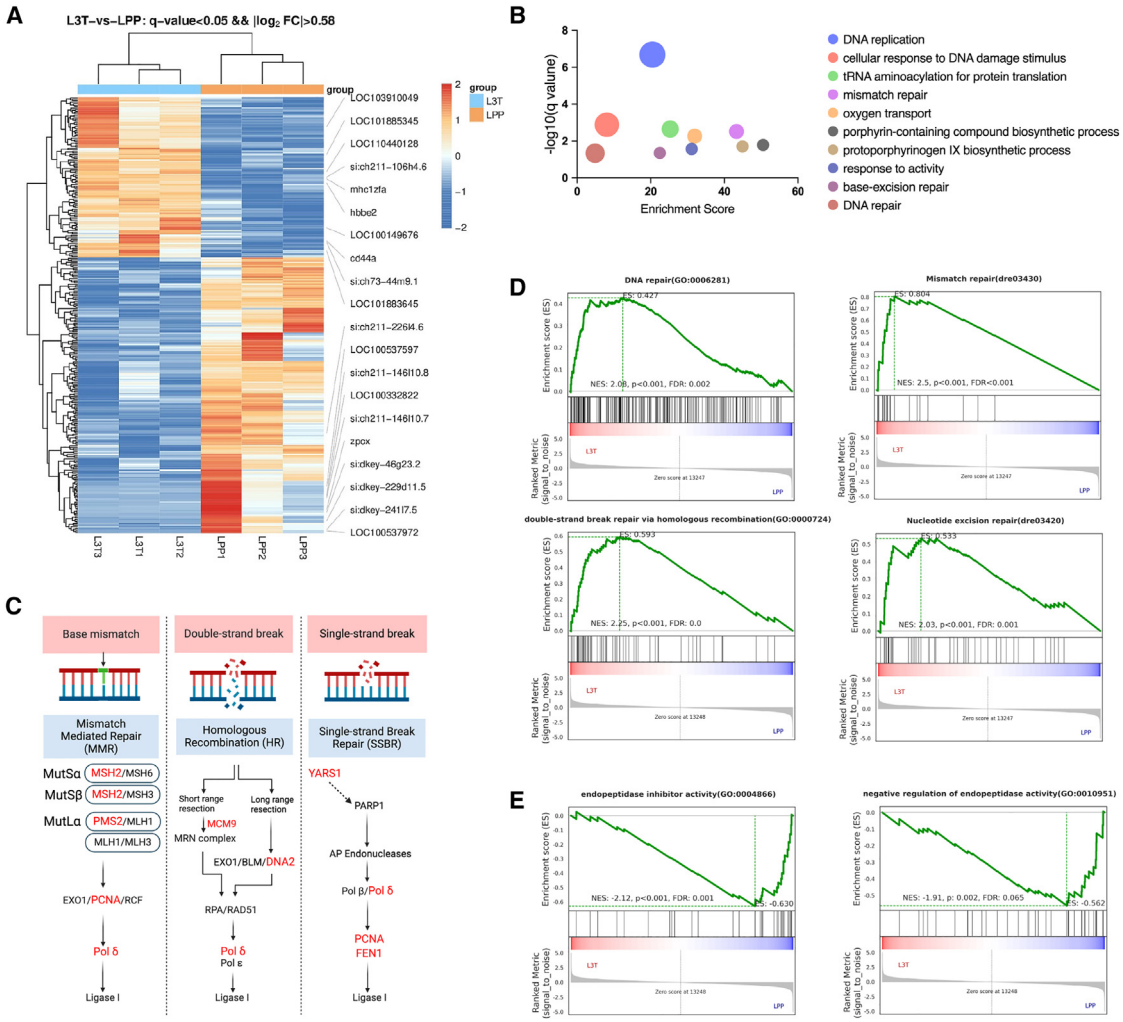

Figure 4. L3T mRNA vaccine induces DNA damage repair

(A) Heatmap of differentially expressed genes (DEGs) of zebrafish immunized with L3T or the LPP control. (B) Enrichment of upregulated genes in the L3T immunized zebrafish by GO analysis. (C) DNA break repair pathways. Genes upregulated in the L3T immunized zebrafish were highlighted in red. (D and E) GSEA of the DEGs in L3T immunized groups compared with the control LPP group.

HR (Figure 4C).[33] MCM9 is a member of the mini-chromosome maintenance (MCM) protein family. The MCM8-MCM9 complex is involved in the HR by recruiting the MRN complex to the repair site[34] and promoting the complex nuclease activity.[35] Long-range resection is primarily executed by EXO1 or by the joint effort of DNA2 and BLM (Figure 4C).[33] DNA2 is a DNA helicase/nuclease that cleaves 5′-single-stranded DNA to generate 3′ overhangs, which commits cells to the HR pathway.[36]

Single-strand breaks (SSBs) are often generated from oxidative damage to DNA. In the long patch SSB repair pathway, PARP1 detects SSBs and initiates the SSB repair pathway.[32] FEN1 is an endonuclease involved in a later step of this pathway, where it removes the damaged 5′ termini (Figure 4C).[32] PCNA and DNA polymerase δ also participate in the SSB repair pathway (Figure 4C). YARS1 acts as a positive regulator of PARP1 (Figure 4C), independently of its tyrosine-tRNA ligase activity, thereby contributing to the SSB repair.[37]

SSRP1a and SPT16 forms the facilitates chromatin transcription complex, which acts as a histone chaperone that both destabilizes and restores nucleosome integrity as part of a chromatin repair system.[38] SPATA18 is a p53-inducible protein, which induces lysosome-like organelles within mitochondria, thereby contributing to mitochondrial quality control.[39]

Gene set enrichment analysis (GSEA) of the DEGs further revealed that the transcripts involved in DNA repair, including mismatch repair, DSB repair, and nucleotide excision repair, were particularly increased in the L3T immunized zebrafish (Figure 4D).

DNA damage repair is essential for maintaining genome stability. Dysregulation of this repair process is associated with cancer susceptibility, accelerated aging, and developmental abnormalities.[40,41] However, it is well documented that deliberate DNA breaks and rearrangements, such as V(D)J recombination, class switch DNA recombination, and somatic hypermutation, that occur in the processes of lymphocyte development, are essential for the generation of a diverse set of immune receptors and antibodies capable of recognizing a broad range of antigens.[42–44] Deficiency in enzymes involved in DNA breaks and repair can lead to immunodeficiency. For example, RAG1 and RAG2 generate DNA DSBs to initiate the V(D)J recombination.[45] RAG1- or RAG2-deficient mice exhibit a severe combined immunodeficiency phenotype, lacking mature B and T cells.[46,47] Additionally, mice deficient in *Psm2* or *Msh2* have a limited B cell repertoire and few somatic mutations at the immunoglobin heavy chain, suggesting that the mismatch repair system contributes to somatic hypermutation rather than suppressing it.[48,49]

The observation that multiple DNA repair systems are activated in the L3T immunized zebrafish suggests that our RNA-seq analysis has captured a snapshot of B cell affinity maturation and T cell activation processes in the normal development of adaptive immunity. Accordingly, genes encoding immunoglobulins (Igs) or Ig-like domain proteins were significantly enriched ($p = 0.04$) among genes upregulated in the L3T-immunized zebrafish. These include *Ighv2-1* (Ig heavy-chain variable 2-1) and *Ighv4-5* (Ig heavy-chain variable 4-5), both predicted to be involved in antigen binding and Ig receptor binding[50]; *Mhc1zfa* (major histocompatibility complex [MHC] class I ZFA), which is involved in antigen presentation to $CD8^+$ T cells; *si:ch211-209L18.4* and *si:ch73-44m9.1*, which encode for Ig-like V-set domains found in Ig light and heavy chains and T cell receptors (CD4, CD80, and CD86); and *LOC100536726* and *LOC101883645*, which encode for uncharacterized Ig-like proteins. These lymphocyte receptor variants likely emerge as a result of selection processes to increase antigen responsiveness, such as B cell affinity maturation[44] and T cell functional avidity maturation,[51,52] and confer high-affinity binding to the L3T antigen.

The gene encoding CD44 (*Cd44a*) is also upregulated in the L3T immunized zebrafish (Figure 4A). CD44 is upregulated shortly after T cell receptor (TCR) engagement and remains expressed on both effector cells and those that survive to become memory cells after the immune response subsides.[53] As such, CD44 is widely used as an indicator of prior antigen exposure and serves as a prominent activation marker, which distinguishes antigen-experienced effector and memory T cells from their naive counterparts.[54]

Consistent with the above evidence of antigen-dependent activation of B and T cell response, genes involved in endopeptidase inhibitor activity and negative regulation of endopeptidase activity were significantly downregulated in the L3T-immunized zebrafish (Figure 4E), indicating increased antigen degradation and processing in this group.

Collectively, these results suggest that L3T mRNA immunization activates canonical DNA damage repair processes, leading to the development of adaptive immunity, including the production of antigen-specific antibodies and T cells.

L3T mRNA vaccine primes autophagy

Autophagy is a catabolic process through which damaged cytoplasmic materials, including proteins and organelles, are delivered to lysosomes for degradation. Autophagy plays a central role in the maintenance of cellular homeostasis and is activated in response to various cell stresses, such as starvation, hypoxia, mitochondrial damage, and pathogen infection.[55] Emerging evidence suggests that DNA damage repair and autophagy may be mechanistically linked, despite occurring in spatially distinct cellular compartments.[56,57] For example, MSH2 and MSH6 of the mismatch repair system acted as sensors of DNA damage induced by 5-fluorouracil. APN-1 and EXO3 of the base excision system acted on the subsequent steps of DNA repair and also activated autophagy.[58] Mitophagy is the process of removing damaged mitochondria by autophagy. Dan et al. recently found that SPATA18, a protein that contributes to mitochondrial quality control, was required for the activation of mitophagy.[59] Knock down of *Spata18* suppressed mitophagy induction and was associated with reduced DNA repair.

The observation that levels of MSH2, PMS2, SPATA18, and cathepsin S, a major protease in lysosomes, were elevated in the L3T-immunized zebrafish promoted a closer examination of autophagy. Reasoning that autophagy would be more readily detected after *M. marinum* challenge, we chose zebrafish that were immunized and then challenged with *M. marinum* for 3 weeks for the analysis (Figure 2E).

LC3, a mammalian homolog of yeast ATG8, is a ubiquitin-like protein that plays a key role in autophagosome formation.[55] Cytosolic LC3 (LC3-I) is conjugated to phosphatidylethanolamine, forming the LC3-II isoform that is tightly associated with both the outer and inner membranes of autophagosomes. In xenophagy and selective autophagy, soluble adaptor protein p62 binds a molecular tag (e.g., polyubiquitin) of intracellular bacteria or endogenous cargo, respectively, and selectively targets them to the $LC3^+$ nascent autophagosome membranes by interacting with LC3-II.[60] Subsequent steps include the formation of the autophagosome and its fusion with lysosomes, in which the autophagosomal contents, including bacteria or cargo, as well as p62 and LC3-II, are degraded. LC3-II bound to the outer membrane of autophagosome is then cleaved and recycled for a new round of lipidation.[60]

We recognize that autophagy is a dynamic process and should ideally be measured in functional assays. However, immunohistochemistry (IHC) is a convenient method for tissue-based analysis. LC3B, an isoform of LC3, and p62 are frequently used as markers to assess autophagy in clinical samples under disease conditions.[55] Dot-like staining of LC3B serves as a surrogate marker for autophagic vesicles, while p62, which is constantly degraded in autolysosomes, acts as a surrogate marker for autophagic degradation.[55]

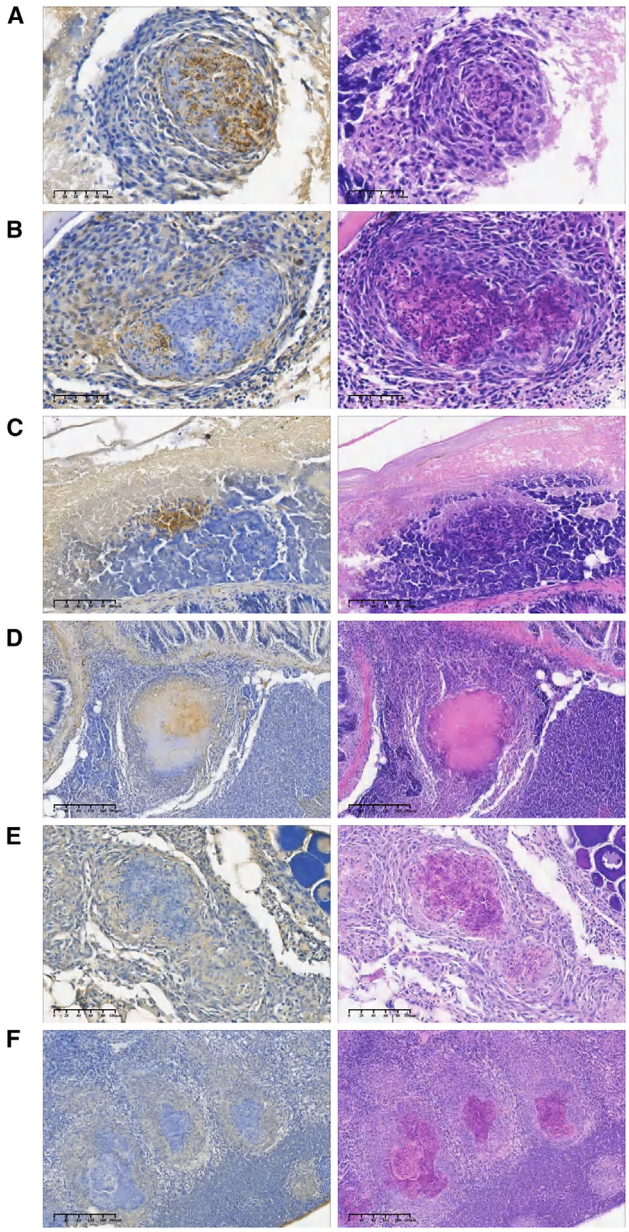

Figure 5. LC3B staining

LC3B immunohistochemical and H&E staining of organs of the L3T group (A–D) and the control groups LPP (E) and PBS (F).

Immunostaining detected a strong signal of LC3B in the granulomas of the L3T-immunized zebrafish (Figure 5). About 10% of granulomas in the L3T group stained positive for LC3B, exhibiting dot-like patterns indicative of autophagosomes (see examples in Figures 5A–5D). Consistent with the pro-survival role of autophagy, LC3B was most strongly and extensively detected in non-necrotizing granulomas (Figure 5A) and was only detected in the peripheral of necrotizing granulomas (Figures 5B and 5C). Interestingly, positive staining of LC3B was even detected in a granuloma with caseous necrosis, albeit at a lower level (Figure 5D). Importantly, none of the granulomas in the control groups (PBS and LPP) stained positive for LC3B, regardless of the level of necrosis (Figures 5E and 5F).

About 50% of the granulomas in the L3T-immunized zebrafish stained positive for p62 and exhibited a range of staining patterns and signal intensities (Figure 6). Strong p62 signal was detected in macrophages that were in immediate contact with bacteria; they formed oval or crescent shapes that completely or partially encircled the area of granulomas populated with bacteria, restricting the dissemination of the pathogen (Figures 6A and 6B). These macrophages exhibited large vacuoles (Figure 6B), and p62 stained strongly at the vacuolar membranes (Figure 6C, arrow). The intensity of the p62 signal correlates closely with the size of the bacterial population. In granulomas with fewer bacteria, the p62 signal was less intense (Figure 6D). Diffuse and weak signals were detected at granulomas that contained no detectable bacteria (Figure 6E). Importantly, the association of the strong p62 signal with the bacterial population was repeatedly observed in the L3T-immunized zebrafish but not in the control groups. In the control groups, only a weak and diffuse signal of p62 was detected, even in granulomas that contained numerous bacteria (Figures 6F and 6G). Together, these observations suggest that in the L3T-immunized zebrafish, macrophages with strong p62 signal were actively engulfing and targeting bacteria for autophagic degradation, as evidenced by their confinement of the bacteria and the appearance of large vacuoles (Figure 6C, arrow). These macrophages likely play a key role in eliminating the invading pathogen. As the bacterial population decreased, fewer macrophages expressing high levels of p62 were needed (Figure 6D), and in granulomas that had completely cleared off bacteria, p62 was degraded and no longer detected (Figure 6E).

The observation that in the L3T group, the p62 signal was not detected in macrophages that were not in direct contact with bacteria suggests that the induction of p62 expression was bacteria dependent. However, the lack of strong p62 signals in bacteria-contacting macrophages in granulomas from the control groups also indicates that the bacteria alone was insufficient to drive p62 expression and required priming by the L3T immunization.

Intriguingly, there was little overlap between the $LC3B^{+}$ and $p62^{+}$ granulomas, which may suggest different kinetics of LC3B and p62 degradation, or alternatively, that a p62-driven and LC3-independent pathway was also activated.[61]

Collectively, these results suggest that the L3T mRNA vaccine successfully induces both innate and adaptive immune mechanisms, leading to the effective control of bacterial infection.

Therapeutic activity of L3T mRNA is mediated by DNA damage repair

To understand the therapeutic mechanisms of the L3T vaccine, we performed RNA-seq analysis of kidneys isolated from zebrafish

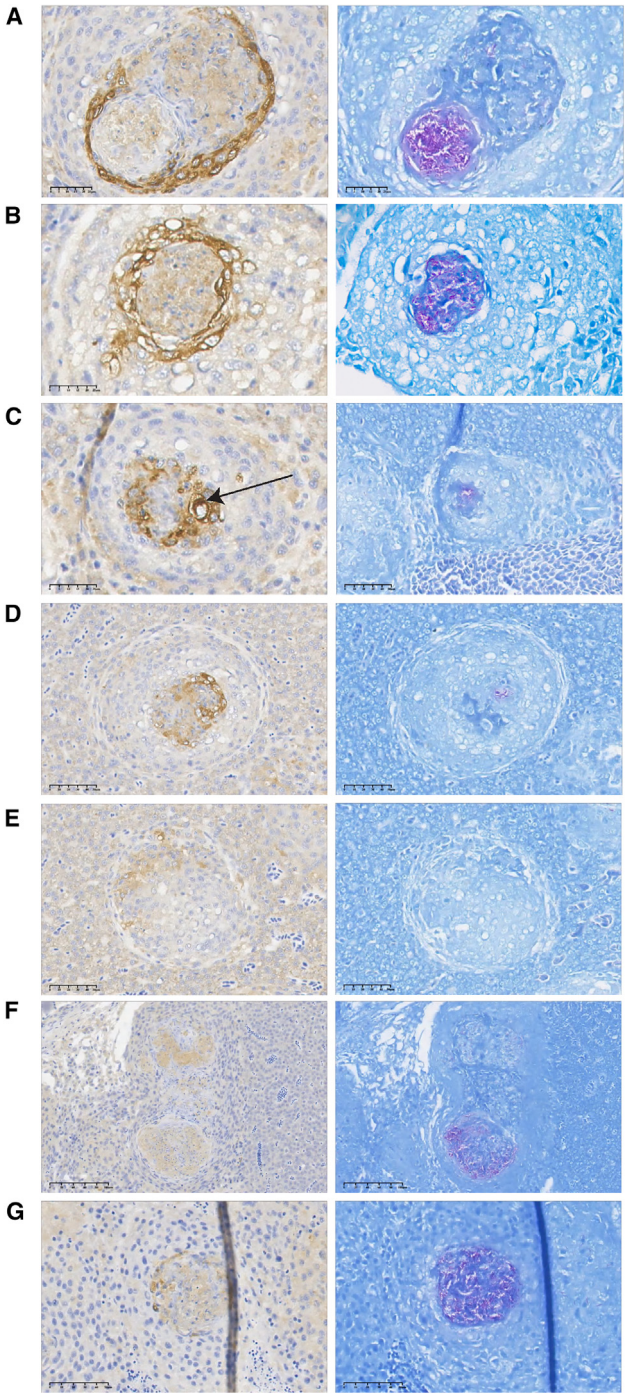

Figure 6. p62 staining

p62 immunohistochemical and acid-fast staining of organs of the L3T group (A–E) and the control groups PBS (F) and LPP (G). The arrow in (C) indicates the strong p62 signal and the association with the large vacuole.

infected with *M. marinum* 535 followed by treatment with L3T mRNA (Figure 3D). We first compared the RNA-seq data of untreated (PBS) zebrafish at 24 dpi with that of zebrafish at 14 dpi to assess the immune change during disease progression. As expected, more upregulated genes (45) than downregulated genes (14) were detected in the immune system category in zebrafish at 24 dpi compared with those at 14 dpi. A majority (38) of the upregulated genes were involved in receptor signaling pathways, including Toll-like receptor signaling, NOD-like receptor signaling, and C-type lectin receptor signaling. Five upregulated genes are involved in the intestinal immune network for IgA production. Comparing the L3T treatment group at 24 and 14 dpi revealed that 36 genes in the immune system category were upregulated in the L3T treatment group, 24 of which overlapped with those in the PBS group. Interestingly, more genes (10) involved in the intestinal immune network for IgA production were upregulated in the L3T group than in the LPP group, suggesting that the L3T vaccine induced adaptive immunity.

We next compared genes involved in inflammation. Twenty-three genes associated with inflammatory response were upregulated in the untreated zebrafish at 24 dpi compared with those at 14 dpi. A similar number of genes (21) were upregulated in the L3T treatment group, 13 of which overlapped with those in the PBS group. The expression levels of these inflammation-associated genes were largely similar between the L3T and the PBS group, except for two chemokine ligand genes (*Ccl38.1* and *Ccl39.2*). Together, these results suggest that the immune response and inflammation caused by bacterial infection were largely unaffected by the subsequent mRNA vaccine treatment.

Strikingly, 52 genes involved in the DNA replication and repair group were downregulated in untreated zebrafish at 24 dpi compared at 14 dpi, while only 2 genes in this category were upregulated. We plotted the log2 ratio of the number of upregulated genes divided by the number of downregulated genes in each category. The genes involved in the DNA replication and repair category were the most downregulated (Figure 7A), suggesting that during the 10-day disease progression, *M. marinum* suppressed the host's DNA damage repair and replication machinery. In contrast, only four genes were downregulated and one gene was upregulated in the DNA replication and repair category in the L3T treatment group, suggesting that L3T treatment was able to counteract the downregulation of DNA replication and repair induced by *M. marinum* infection (Figure 7A). Comparison of the DEGs of the L3T treatment group and the PBS group at the same time point (24 dpi) also revealed that genes involved in DNA replication (Figure 7B) and repair pathways (Figures 7C–7F) were positively enriched. A similar result was obtained when comparing the L3T treatment group and the LPP control group. Taken together, these data suggest that during natural disease progression, inflammation caused by bacterial infection induced DNA damage; however, *M. marinum* managed to suppress the host DNA damage repair and replication systems, which led to the death of the zebrafish. In contrast, L3T treatment activated the host DNA damage repair and replication systems and largely neutralized the negative effect of the pathogen, thereby prolonging the survival of the zebrafish (Figure 3E).

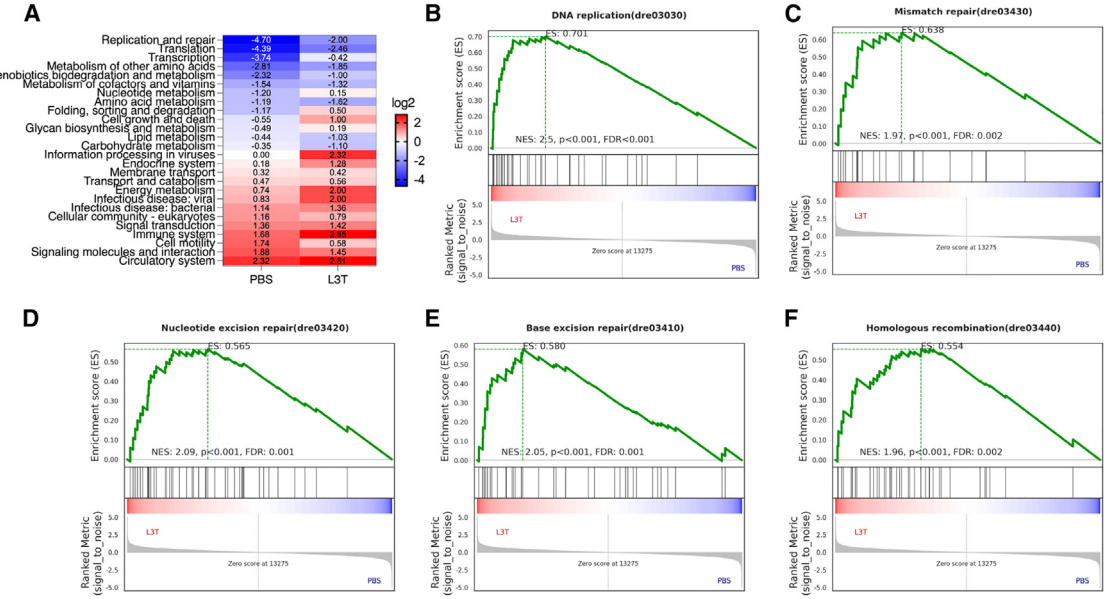

Figure 7. RNA-seq analysis of zebrafish infected with *M. marinum* 535 and treated with L3T mRNA

(A) Significantly enriched KEGG pathways and the log2 ratio of the number of upregulated genes/the number of downregulated genes in each pathway. PBS, compared zebrafish at 24 days post-infection with those at 14 days post-infection; L3T, compared L3T treatment group at 24 days post-infection with those at 14 days post-infection (see Figure 3D). (B–F) GSEA of the DEGs in the L3T treatment group compared with the control PBS group.

DISCUSSION

The role of autophagy as part of the host defense mechanism against *M. tb* infection was initially demonstrated in isolated macrophages[62] and later confirmed in murine models, where mice with conditional knockouts in multiple autophagy genes exhibit increased susceptibility to *M. tb*.[63] In addition to canonical autophagy, recent studies also suggest a non-canonical process, LC3-associated phagocytosis, in the control of *M. tb*.[64–66] This recent evidence and numerous previous studies[67] strongly suggest that autophagy is essential for the control of TB. As such, developing new therapies or vaccines by harnessing autophagy is an area of interest and ongoing effort. Here, we report that an mRNA vaccine delivered by lipid nanoparticles induces macrophage autophagy, as well as B and T cell immunity, and demonstrates superior prophylactic and therapeutic activities, highlighting the requirement of eliciting both innate and adaptive immunity for the control of mycobacterial infection. Our observation of strong p62 signals in macrophages engaged in bacterial killing is consistent with previous *in vitro* studies. Ponpuak et al. showed that p62 was required for autophagic killing of *M. tb* in isolated macrophages.[68] Bone marrow-derived macrophages from p62 knockout mice killed *M. tb* less efficiently upon starvation to activate autophagy. P62 mediated bacterial killing either by delivering ubiquitinated cytosolic proteins to autolysosomes, where they were proteolytically converted into antimicrobial peptides capable of killing *M. tb* sequestered in phagosomes,[68] or by delivering ubiquitinated cytosolic *M. tb* to autophagosomes, followed by lysosome fusion and autolysosome killing.[69] Like *M. tb*, *M. marinum* can escape from phagosomes into the cytosol and be ubiquitinated. p62-mediated autophagy of the ubiquitinated *M. marinum* was demonstrated recently in zebrafish larvae.[70] We propose a similar mechanism in adult zebrafish immunized with the L3T mRNA vaccine. Thus, the synthesis of the L3T antigen in the cytosol activates the ubiquitin-proteasome system (UPS), which degrades the antigen, and the resulting peptides are translocated to the endoplasmic reticulum to access MHC class I for antigen presentation.[71] The activated UPS also mediates the ubiquitination of cytosolic *M. marinum*, which is then targeted by p62 for autophagic degradation. Supporting this, several genes encoding proteins with predicted ubiquitin ligase or transferase activity were upregulated in the L3T-immunized zebrafish, including *the RING domain-containing E3 ligases Trim35-7*, *Rnf26*, *and Rnf122*. It is well documented that there are multiple crosstalks between members of the UPS and autophagy,[72,73] the two major cellular pathways for protein degradation. For example, TRIM16 activates the expression and interacts with p62, thereby facilitating autophagic degradation of protein aggregates.[74] RNF26 plays a key role in regulating the spatiotemporal positioning of endosomes in cells by directly recruiting and ubiquitinating p62.[75] Whether this interaction converges or plays a role in autophagy remains to be determined in future studies.

Programmed DNA DSBs and rearrangements take place in adaptive immune cells during the assembly and diversification of lymphocyte antigen receptor genes, in the process of V(D)J recombination,[42,43] including the immunoglobin heavy-chain genes and light-chain κ and λ genes of B cells, as well as the TCR-β, -α, -γ, and -δ chain genes. Somatic hypermutation introduces non-templated point mutations at an extremely high rate ($\sim 10^{-3}$ mutations per base pair per cell division) in the variable region of immunoglobin genes.[76] This process

drives affinity maturation, which results in the expansion of B cells expressing an immunoglobin that has high affinity for its cognate antigen.[76] These deliberate DNA breaks and rearrangements are essential for normal lymphocyte development. As such, it is not surprising that multiple genes involved in canonical DNA repair systems, including mismatch repair and DSB and SSB repairs, were enriched and upregulated in the L3T mRNA immunized zebrafish. We consider this to be evidence of the successful induction of B cell and T cell immunity. This is further supported by the enrichment and upregulation of specific alleles of immunoglobin heavy-chain genes and TCR genes, as well as the excellent antimycobacterial activity mediated by the L3T immunization.

DNA damage generated by endogenous processes or exogenous genotoxic agents, such as ionizing radiation and genotoxic drugs, activates multiple cellular response programs. These include the well-documented canonical p53-mediated transcriptional program, which primarily promotes cell-cycle arrest and apoptosis in cells with extensive or persistent DNA breaks,[77] and the more recently discovered cyclic guanosine monophosphate (GMP)-AMP synthase (cGAS)-stimulator of interferon genes (STING) innate immune signaling pathway, which responds to damaged nuclear DNA, cytosolic endogenous DNA, or foreign DNA.[78] Studies by Sleckman and co-workers have identified an additional signaling pathway that responds to DNA damage occurring under more physiologically relevant conditions, such as RAG-mediated DNA DSBs in the process of V(D)J recombination. These non-canonical DNA damage responses regulate cell-type-specific processes essential for the normal development and function of innate and adaptive immunity.[79,80] It is unclear how cells choose between this pro-survival pathway and the p53-mediated signaling pathway that promotes cell death. Interestingly, the p53-mediated signaling pathway and the cGAS-STING signaling pathway were not activated in zebrafish by the L3T mRNA immunization; there was no enrichment of genes involved in these pathways by GO and Kyoto Encyclopedia of Genes and Genomes (KEGG) analysis, as opposed to genes involved in DNA damage repair and replication. Our results suggest that during the natural process of immunization, the host may minimize the pro-death DNA damage response, such as the p53 signaling, to prevent unwanted apoptosis of developing lymphocytes that would otherwise undergo successful receptor gene assembly. Instead, the host favors pro-survival pathways that are essential for normal lymphocyte development. This is also consistent with our observation that the L3T mRNA vaccine is generally safe and well tolerated.

It is remarkable that the L3T mRNA vaccine demonstrated exceptionally potent bactericidal activity, surpassing that of the first-line antibiotic rifampicin when administered post-infection. To our knowledge, such efficiency has not been described previously for a TB vaccine. One possible explanation is that the lysin B encoded by the L3T mRNA contributed to bacterial killing. However, as mRNA transcript levels declined rapidly and reached background levels 72 h after injection,[81] the contribution of lysin B protein in bacterial killing could be limited. Nonetheless, our work demonstrated the versatility of the mRNA platform, and future studies aimed at improving mRNA stability and abundance (e.g., self-amplifying RNA) are warranted.

MATERIALS AND METHODS

Zebrafish

The wild-type adult zebrafish (*Danio rerio* AB strain, 3–4 months old) were obtained from Nanjing Yishulihua Biotechnology, and husbandry was performed as previously described.[30] Tg(*lyz::DsRed*) and Tg(*mpeg1::LRLG*) were obtained from Dr. Bo Yan. All fish larvae, except for survival experiments, were placed in egg water with 0.22 μM *N*-phenylthiourea (Sigma-Aldrich) to prevent the formation of pigments and maintained as previously described.[82]

Bacteria and cell lines

M. marinum cultures were grown at 30°C in Middlebrook 7H9 broth (Becton Dickinson, catalog no. 271310) or 7H10 agar (Becton Dickinson, catalog no. 262710) supplemented with 0.2% glycerol (7H9) or 0.5% glycerol (7H10), 0.05% Tween 80, and 10% oleic acid albumin dextrose catalase.

HEK293T (ATCC CRL-3216) was purchased from the National Collection of Authenticated Cell Cultures. Adherent cells were cultured in DMEM supplemented with 1% penicillin/streptomycin (Thermo Fisher) and 10% fetal bovine serum (Thermo Fisher).

Production of recombinant GlnA1 protein and anti-GlnA1 antibody

Recombinant protein GlnA1 was produced and purified as described previously.[83] Briefly, the DNA fragment of *M. tb glnA1* (*Rv2220*) was amplified by PCR using specific primers and inserted into pET28a to generate the recombinant pET28a-Rv2220. Sequence correct pET-28a-Rv2220 plasmid was transformed into *Escherichia coli* BL21. Protein expression was induced with 1 mM isopropyl thiogalactoside and GlnA1 protein was purified using Ni-nitrilotriacetic acid His•Bind Resin (Novagen). Purified proteins were desalted using PD-10 Desalting Column (Cytiva), and the endotoxin was removed using the ToxinEraser Endotoxin Removal Kit (Genscript). New Zealand rabbits were immunized with the purified GlnA1 emulsified with Freund's adjuvant three times, and antisera were obtained and purified by protein A/G.

The production of pcDNA-L3 and L3 mRNA

The fusion antigen L3 is composed of two antigens: LysB-GlnA1 (Figure 1A), and the thrombin recognition and cleavage site with nine amino acids (GGACTAGTACCCCGAGGATCAACAGGA, GLVPR GSTG) was introduced as the linker of these two antigens. The full-length DNA fragment of L3 was amplified by PCR using specific primers and inserted into the pcDNA3.1+ expression vector. The Kozak sequence (GCCACC) was added before the start codon of L3 to increase the expression of antigen. The DNA construct was sequenced and purified with EndoFree Maxi Plasmid Kit (TIANGEN) prior to transfection and injection. To enhance mRNA stability and

translation efficiency, the open reading frame sequence of L3 and Ag85a was codon optimized for humans using the codon optimization tTool from Thermo Fisher (https://www.thermofisher.com/order/geneartgenes/projectmgmt), Genscript (https://www.genscript.com/tools/gensmart-codon-optimization), DnaChisel (https://github.com/Edinburgh-Genome-Foundry/DnaChisel).

mRNA was produced using T7 RNA polymerase on linearized plasmids encoding codon-optimized L3 protein. The plasmid was linearized using the restriction endonuclease BspQI (NEB, catalog no. R0712L). mRNA was transcribed to contain a 75-nt-long poly(A) tail, with 100% of uridine triphosphate (UTP) substituted with 1-methylpseudo-UTP to produce m1Ψ-modified mRNA. The m7G (5′) ppp (5′) G RNA Cap Structure Analog was used for co-transcriptional capping of mRNAs. The modified mRNAs included a 5′ Cap1, a 5′ UTR of the *X. laevis* β-globin gene, a coding region for L3, a 3′ UTR of the human α-globin gene, and a poly(A) tail (Figure 1A). mRNA was purified by overnight LiCl precipitation at −20°C, centrifuged at 18,800 × *g* for 20 min at 4°C to pellet, washed with 70% EtOH, centrifuged at 18,800 × *g* for 1 min at 4°C, and resuspended in RNase-free water. Purified mRNA was analyzed by agarose gel electrophoresis and stored at −80°C until further use.

LPP nanoparticles were prepared using the two-step method described previously.[26,81] In brief, the cationic compound (SW-01) was dissolved in 25 mM sodium acetate (pH 5.2) to prepare an SW-01 solution (0.5 mg/mL). The mRNA solution (0.1 μg/μL) and SW-01 solution were quickly stirred and mixed according to the volume ratio of 5:1 and then stood at room temperature for 30 min to form the mRNA/SW-01 complex. Then, lipids were dissolved in ethanol at molar ratios of 40:15:43.5:1.5 (ionizable lipid: 1,2-dioleoyl-*sn*-glycero-3-phosphoethanolamine:cholesterol:polyethylene glycol-lipid). The lipid solution was blended with the mRNA/SW-01 complexes using a microfluidic mixer (Inano D, Micro&Nano Technology) at a proportion of three parts aqueous phase to one part ethanol phase. Finally, LPP-L3 mRNA was sterilized with a 0.22-μm filter (Millipore) and stored at 4°C with an RNA concentration of about 1 mg/mL; it was stored at −80°C for no more than 1 year for later use.

DNA and mRNA transfection *in vitro*

For DNA and mRNA transfection into HEK293T, 2.5×10^5 cells per well were seeded in 12-well plates. DNA, 2.5 μg, was transfected into HEK293T cells using Lipofectamine8000 transfection kits (Beyotime, catalog no. C0533) according to the manufacturer's instructions. mRNA vaccine, 2.5 μg, was transfected into HEK293T. At 24 h after transfection, cells were lysed with radioimmunoprecipitation assay (RIPA) lysis buffer (Beyotime, catalog no. P0013B). Supernatant was collected to detect the expression of L3. Anti-GlnA1 polyclonal antibody and goat anti-mouse IgG(H + L) secondary antibody, horseradish peroxidase (HRP) linked, was used for western blot analysis. Glyceraldehyde 3-phosphate dehydrogenase (GAPDH) was used as the endogenous control, and the pcDNA 3.1 empty vector or LPP were transfected as the negative control.

DNA and mRNA immunization regimens

For the assessment of *in vivo* mRNA expression, 3-dpf (day post-fertilization) wild-type embryos were i.m. injected with 3 ng per fish of LPP-mRNA candidate vaccines. After a 24-h injection, the fish were sacrificed and lysed with RIPA lysis buffer (Beyotime, catalog no. P0013B). Supernatant was collected to detect the expression of L3.

For mRNA candidate vaccine safety assessment, 3-dpf wild-type embryos were i.m. injected with different concentrations of LPP-mRNA candidate vaccines. Feeding started at 5 dpf with a dry larval diet (Zeigler, catalog no. AP100) twice per day, and death of the embryos was monitored daily until 13 dpf.

For the mRNA injection-induced macrophage and neutrophil recruitment assay, embryos were pre-treated with propylthiouracil 48 h before the assays. Zebrafish embryos, 3 dpf, were anesthetized with tricaine (Sigma, 200 μg/mL) and mounted in 1% low-melting-point agarose for i.m. injection with 3 ng mRNA candidate vaccines in the dorsal muscle.

To investigate the prophylactic activity of DNA or mRNA vaccines, adult zebrafish (AB strain, 3–4 months old) were immunized twice with 2-week intervals (weeks 0 and 2). Dose volumes were 2 μL for i.m. immunization. For DNA vaccination, L3 DNA vaccine was injected with 6 μg DNA in the dorsal muscle using PV830 Pneumatic PicoPump microinjector (World Precision Instruments), and the target tissue was electroporated (6 pulses of 50 V, 5 ms each) using tweezer-type electrodes (BTX/Harvard Apparatus) and a GenePulser-electroporator (Bio-Rad). Injection with pcDNA3.1 plasmid was used as a negative control.

For mRNA vaccination, mRNA candidate vaccines were injected with 1 μg LPP-mRNA in the dorsal muscle using the PV830 Pneumatic PicoPump microinjector (World Precision Instruments), and the negative control zebrafish were immunized with LPP-GFP mRNA or sterile PBS.

To investigate the therapeutic activity of the L3 mRNA vaccine, 3-dpf wild-type embryos were infected with *M. marinum* 535:GFP and i.m. injected with 3 ng mRNA candidate vaccines in the dorsal muscle at 24 h post-infection. Feeding started at 5 dpf with a dry larval diet (Zeigler, catalog no. AP100) twice per day, and death of the embryos was monitored daily until 13 dpf. Adult zebrafish (AB strain, 3–4 months old) were infected with indicated *M. marinum* strains for 2 weeks. They were then injected twice with 3-day intervals (days 14 and 17) of the L3T mRNA (0.5 μg) at the dorsal muscle using the PV830 Pneumatic PicoPump microinjector, and the negative control zebrafish were immunized with LPP-GFP mRNA or sterile PBS. Rifampicin (400 μM) was administered through a chronic bath for 7 days and used as the positive control. The therapeutic effect of combining L3T mRNA vaccine with rifampicin treatment was also evaluated in this study.

M. marinum infections

Adult zebrafish infection with *M. marinum* was performed as described previously.[30] Briefly, for studies of the therapeutic activity of the L3T mRNA, adult zebrafish (AB strain, 3–4 months old) were anesthetized in 0.1% tricaine and infected by intraperitoneal injection of *M. marinum* 1218R or the *whiB4* inactivated strain (*whiB4*:Tn) of *M. marinum* 1218R at 10^4 colony-forming units (CFU) bacteria per fish, or Rif^R of *M. marinum* 535 at 10^2 CFU bacteria per fish, or *M. marinum* 535 at 30 CFU bacteria per fish.

For studies of the prophylactic activity of the L3T mRNA, 4 weeks after the second immunization, adult zebrafish (AB strain, 3–4 months old) were anesthetized in 0.1% tricaine and infected by intraperitoneal injection of *M. marinum* 535 at 500 CFU bacteria per fish or PBS as the negative control and monitored for their survival.

For zebrafish larvae infection with *M. marinum*, zebrafish embryos (3 dpf) were anesthetized by adding tricaine (Sigma, catalog no. 886-86-2) and sucked onto an injection plate lined with 1% low melting point agarose. Then, infections were performed by microinjection of *M. marinum* 535:*gfp* (130 CFU) via the duct of Cuvier.

To determine the bacterial burden in adult zebrafish, fish were sacrificed and incubated with 75% ethanol for 5 min to kill bacteria on the surface. They were then rinsed with sterile PBS and homogenized in sterile PBS with Tween 20 using the NOVAprep DS1000 (NewZongKe) at 5,000 rpm for four 30-s cycles with 300-s pauses. The homogenates were diluted and plated to determine the CFU of *M. marinum*.

Histopathology

For histopathological analysis, fish of the protective efficiency evaluation group were sacrificed at 3 weeks post-infection, and fish of the therapeutic efficiency evaluation group were sacrificed at 24 dpi. Fish were fixed in 10% phosphate-buffered formalin for 7 days and then decalcified with 20% EDTA-citrate for 7 days. After dehydration with ethanol, specimens were placed in xylene and embedded in paraffin; then, 4-μm serial paraffin sections were prepared and subjected to H&E staining, Ziehl-Neelsen acid fast staining and IHC staining as previously described.[30] For IHC staining, anti-SQSTM1/p62 rabbit polyclonal antibody (pAb; Servicebio, GB11531) and anti-LC3B rabbit pAb (AiFang Biological, AFW11923) were used in this study.

Microscopy

For quantification of bacterial burdens, after the larvae were immunized with L3T mRNA, fish were divided into 48-well plates. At 3 and 4 dpi, the therapeutic efficacy of the mRNA vaccine was assessed by monitoring the fluorescent bacterial burden in the tail region of the larvae using the fluorescence microscopy imaging system. Fluorescent images were taken with a Leica fluorescence microscope. Bacterial burden was quantified by measuring the integrated fluorescent intensity of labeled bacteria with ImageJ software.

For evaluation of macrophage and neutrophil recruitment induced by the L3T mRNA vaccine injected, a Leica confocal microscope with a 4× Plan Apo 0.75 numerical aperture objective was used to generate 10-μm z stacks with 1-μm step size. Time-lapse images were taken at 2- to 10-min intervals for 4 h. Data were acquired with LAS X FLIM FCS (Leica), and movies were exported from ImageJ software for the addition of labels and stitching. And at 4 and 24 h post-injection, the macrophage and neutrophil recruitment efficiencies were assessed by monitoring fluorescent cells in the injection region of larvae using the fluorescence microscopy imaging system. Fluorescent images were taken by a Leica fluorescence microscope. Recruitment efficiency was quantified by measuring the integrated fluorescent intensity of labeled cells with ImageJ software.

RNA-seq and analysis

For determination of the host immune response induced by mRNA vaccine immunization, adult zebrafish (AB strain, 3–4 months old, 15 per group) were immunized twice with 2-week intervals (weeks 0 and 2). Dose volumes were 2 μL for i.m. immunization. L3T mRNA vaccine, 1 μg, or LPP-GFP mRNA were injected in the dorsal muscle using the PV830 Pneumatic PicoPump microinjector. After 12 days of the secondary immunization, the kidneys of the adult zebrafish were isolated and placed in 1 mL Trizol for RNA extraction.

To understand the immune therapeutic mechanisms mediated by the L3T vaccine, we performed RNA-seq analysis of kidneys isolated from *M. marinum* 535-infected zebrafish (AB strain, 3–4 months old, 15 per group) treatment with the L3T mRNA vaccine and the LPP control, PBS control, and without treatment control (infection 14 days), as well as healthy controls. Adult zebrafish (AB strain, 3–4 months old) were infected with the indicated *M. marinum* 535 at 30 CFU bacteria per fish for 2 weeks and were then injected twice with 3-day intervals (days 14 and 17) of the L3T mRNA (0.5 μg) at the dorsal muscle using the PV830 Pneumatic PicoPump microinjector, and negative control zebrafish were immunized with LPP-GFP mRNA or sterile PBS. After 7 days of the final immunization, kidneys from five zebrafish were pooled as one sample, and three samples (total of 15 kidneys) collected for each group were subjected to RNA-seq analysis. We also collected the zebrafish kidneys infected with *M. marinum* 535 strain 14 days before treatment to RNA-seq and healthy kidneys as blank control.

Fifteen kidneys per group were collected and pooled as three samples. The cDNA library construction, Illumina sequencing, and transcriptome expression analysis were performed as described previously.[30]

Western blot

For cells transfected with DNA or mRNA vaccine, after 24 h of transfection, cell culture medium was removed, and cell pellets were washed with PBS and collected into 1.5-mL Eppendorf tubes. For larvae immunized with mRNA vaccine, after 24 h of immunization, 30 larvae zebrafish per group were euthanized and collected into 1.5-mL Eppendorf tubes. Then, 150 μL RIPA lysis buffer (Beyotime, catalog no. P0013B) containing protease inhibitor cocktail (Beyotime,

catalog no. P1005) was added, lysed at 4°C on a shaker for 30 min, and centrifuged (4°C, 12,000 × *g*, 30 min), and the supernatant was collected. An appropriate volume of 5× loading buffer was added and boiled in a metal bath at 95°C for 10 min. The protein samples were separated by SDS-PAGE, and the presence of L3 and GAPDH were assayed by western blot using the following antibodies: rabbit anti-GlnA1 Ab (1:500, this study), rabbit-anti GAPDH Ab (1:3000, Sangon), and goat anti-mouse IgG(H + L) secondary antibody, HRP linked (1:3,000, Abcam).

DATA AND CODE AVAILABILITY

Raw data of RNA-seq can be retrieved using the GEO platform numbers GSE269547 and GSE270105.

ACKNOWLEDGMENTS

This work was supported by the National Key Research and Development Program of China (2021YFC2301500 and 2018YFD0500900), the National Natural Science Foundation of China (82272353), the Joint Funds of the National Natural Science Foundation of China (U23A20237), and the Shanghai 2020 "Science and Technology Innovation Action Plan" Technological Innovation Fund (20Z11900500). All zebrafish were raised under standard conditions in compliance with laboratory animal guidelines for the ethical review of animal welfare (GB/T 35823-2018). All zebrafish experiments were approved by the local animal care committees at Fudan University.

AUTHOR CONTRIBUTIONS

L.Z., D.C., and J.L. conceived the study. L.Z., J.L., and B.Y. jointly supervised the study. D.C. and W.H. performed the experiments and analyzed the results. Y.L., G.L., L.S., J.Z., Z.Z., and Z.P. assisted in the antigen assessment assays. C.Z., G.L., Y.T., and J.Z. assisted in the animal experiments. S.Z., S.X., J.T., and M.Z. participated in the immune mechanism evaluation experiments. Y.F., F.Z., L.H., and H.L. generated and optimized the mRNA preparations. H.Y. and W.S. participated in the mycobacteria cultivation. Y.L. and H.L. analyzed the immune pathological reactions. J.L., D.C., and L.Z. wrote the paper. All authors have reviewed and approved the paper.

DECLARATION OF INTERESTS

The authors declare no competing interests.

SUPPLEMENTAL INFORMATION

Supplemental information can be found online at https://doi.org/10.1016/j.omtn.2024.102402.

REFERENCES

1. Cohen, A., Mathiasen, V.D., Schon, T., and Wejse, C. (2019). The global prevalence of latent tuberculosis: a systematic review and meta-analysis. Eur. Respir. J. *54*, 1900655.
2. Bagcchi, S. (2023). WHO's Global Tuberculosis Report 2022. Lancet Microbe *4*, e20.
3. Trunz, B.B., Fine, P., and Dye, C. (2006). Effect of BCG vaccination on childhood tuberculous meningitis and miliary tuberculosis worldwide: a meta-analysis and assessment of cost-effectiveness. Lancet *367*, 1173–1180.
4. Mangtani, P., Abubakar, I., Ariti, C., Beynon, R., Pimpin, L., Fine, P.E.M., Rodrigues, L.C., Smith, P.G., Lipman, M., Whiting, P.F., and Sterne, J.A. (2014). Protection by BCG vaccine against tuberculosis: a systematic review of randomized controlled trials. Clin. Infect. Dis. *58*, 470–480.
5. Dos Santos, P.C.P., Messina, N.L., de Oliveira, R.D., da Silva, P.V., Puga, M.A.M., Dalcolmo, M., Dos Santos, G., de Lacerda, M.V.G., Jardim, B.A., de Almeida, E.V.F.F., et al. (2024). Effect of BCG vaccination against Mycobacterium tuberculosis infection in adult Brazilian health-care workers: a nested clinical trial. Lancet Infect. Dis. *24*, 594–601.
6. Colditz, G.A., Brewer, T.F., Berkey, C.S., Wilson, M.E., Burdick, E., Fineberg, H.V., and Mosteller, F. (1994). Efficacy of BCG vaccine in the prevention of tuberculosis. Meta-analysis of the published literature. JAMA *271*, 698–702.
7. Schrager, L.K., Vekemens, J., Drager, N., Lewinsohn, D.M., and Olesen, O.F. (2020). The status of tuberculosis vaccine development. Lancet Infect. Dis. *20*, e28–e37.
8. Tait, D.R., Hatherill, M., Van Der Meeren, O., Ginsberg, A.M., Van Brakel, E., Salaun, B., Scriba, T.J., Akite, E.J., Ayles, H.M., Bollaerts, A., et al. (2019). Final Analysis of a Trial of M72/AS01(E) Vaccine to Prevent Tuberculosis. N. Engl. J. Med. *381*, 2429–2439.
9. Watt, J., and Liu, J. (2020). Preclinical Progress of Subunit and Live Attenuated Mycobacterium tuberculosis Vaccines: A Review following the First in Human Efficacy Trial. Pharmaceutics *12*, 848.
10. Grode, L., Seiler, P., Baumann, S., Hess, J., Brinkmann, V., Nasser Eddine, A., Mann, P., Goosmann, C., Bandermann, S., Smith, D., et al. (2005). Increased vaccine efficacy against tuberculosis of recombinant Mycobacterium bovis bacille Calmette-Guerin mutants that secrete listeriolysin. J. Clin. Invest. *115*, 2472–2479.
11. Martin, C., Williams, A., Hernandez-Pando, R., Cardona, P.J., Gormley, E., Bordat, Y., Soto, C.Y., Clark, S.O., Hatch, G.J., Aguilar, D., et al. (2006). The live Mycobacterium tuberculosis phoP mutant strain is more attenuated than BCG and confers protective immunity against tuberculosis in mice and guinea pigs. Vaccine *24*, 3408–3419.
12. Ahn, S.K., Tran, V., Leung, A., Ng, M., Li, M., and Liu, J. (2018). Recombinant BCG Overexpressing phoP-phoR Confers Enhanced Protection against Tuberculosis. Mol. Ther. *26*, 2863–2874.
13. Hou, X., Zaks, T., Langer, R., and Dong, Y. (2021). Lipid nanoparticles for mRNA delivery. Nat. Rev. Mater. *6*, 1078–1094.
14. Rohner, E., Yang, R., Foo, K.S., Goedel, A., and Chien, K.R. (2022). Unlocking the promise of mRNA therapeutics. Nat. Biotechnol. *40*, 1586–1600.
15. Chaudhary, N., Weissman, D., and Whitehead, K.A. (2021). mRNA vaccines for infectious diseases: principles, delivery and clinical translation. Nat. Rev. Drug Discov. *20*, 817–838.
16. Larsen, S.E., Erasmus, J.H., Reese, V.A., Pecor, T., Archer, J., Kandahar, A., Hsu, F.C., Nicholes, K., Reed, S.G., Baldwin, S.L., and Coler, R.N. (2023). An RNA-Based Vaccine Platform for Use against Mycobacterium tuberculosis. Vaccines (Basel) *11*, 130.
17. Rais, M., Abdelaal, H., Reese, V.A., Ferede, D., Larsen, S.E., Pecor, T., Erasmus, J.H., Archer, J., Khandhar, A.P., Cooper, S.K., et al. (2023). Immunogenicity and protection against Mycobacterium avium with a heterologous RNA prime and protein boost vaccine regimen. Tuberculosis *138*, 102302.
18. Cronan, M.R., and Tobin, D.M. (2014). Fit for consumption: zebrafish as a model for tuberculosis. Dis. Model. Mech. *7*, 777–784.
19. Tullius, M.V., Harth, G., and Horwitz, M.A. (2003). Glutamine synthetase GlnA1 is essential for growth of Mycobacterium tuberculosis in human THP-1 macrophages and guinea pigs. Infect. Immun. *71*, 3927–3936.
20. Harth, G., Clemens, D.L., and Horwitz, M.A. (1994). Glutamine synthetase of Mycobacterium tuberculosis: extracellular release and characterization of its enzymatic activity. Proc. Natl. Acad. Sci. USA *91*, 9342–9346.
21. Hurst-Hess, K., Walz, A., Yang, Y., McGuirk, H., Gonzalez-Juarrero, M., Hatfull, G.F., Ghosh, P., and Ojha, A.K. (2023). Intrapulmonary Treatment with Mycobacteriophage LysB Rapidly Reduces Mycobacterium abscessus Burden. Antimicrob. Agents Chemother. *67*, e0016223.
22. Falcone, D., and Andrews, D.W. (1991). Both the 5' untranslated region and the sequences surrounding the start site contribute to efficient initiation of translation *in vitro*. Mol. Cell Biol. *11*, 2656–2664.
23. Conry, R.M., LoBuglio, A.F., Wright, M., Sumerel, L., Pike, M.J., Johanning, F., Benjamin, R., Lu, D., and Curiel, D.T. (1995). Characterization of a messenger RNA polynucleotide vaccine vector. Cancer Res. *55*, 1397–1400.
24. Andries, O., Mc Cafferty, S., De Smedt, S.C., Weiss, R., Sanders, N.N., and Kitada, T. (2015). N(1)-methylpseudouridine-incorporated mRNA outperforms pseudouridine-incorporated mRNA by providing enhanced protein expression and reduced immunogenicity in mammalian cell lines and mice. J. Control. Release *217*, 337–344.
25. Nance, K.D., and Meier, J.L. (2021). Modifications in an Emergency: The Role of N1-Methylpseudouridine in COVID-19 Vaccines. ACS Cent. Sci. *7*, 748–756.

26. Persano, S., Guevara, M.L., Li, Z., Mai, J., Ferrari, M., Pompa, P.P., and Shen, H. (2017). Lipopolyplex potentiates anti-tumor immunity of mRNA-based vaccination. Biomaterials *125*, 81–89.

27. Awate, S., Babiuk, L.A., and Mutwiri, G. (2013). Mechanisms of action of adjuvants. Front. Immunol. *4*, 114.

28. Basaraba, R.J. (2008). Experimental tuberculosis: the role of comparative pathology in the discovery of improved tuberculosis treatment strategies. Tuberculosis *88*, S35–S47.

29. Davis, J.M., and Ramakrishnan, L. (2009). The role of the granuloma in expansion and dissemination of early tuberculous infection. Cell *136*, 37–49.

30. Lin, C., Tang, Y., Wang, Y., Zhang, J., Li, Y., Xu, S., Xia, B., Zhai, Q., Li, Y., Zhang, L., and Liu, J. (2022). WhiB4 Is Required for the Reactivation of Persistent Infection of Mycobacterium marinum in Zebrafish. Microbiol. Spectr. *10*, e0044321.

31. Menke, A.L., Spitsbergen, J.M., Wolterbeek, A.P.M., and Woutersen, R.A. (2011). Normal anatomy and histology of the adult zebrafish. Toxicol. Pathol. *39*, 759–775.

32. Chatterjee, N., and Walker, G.C. (2017). Mechanisms of DNA damage, repair, and mutagenesis. Environ. Mol. Mutagen. *58*, 235–263.

33. Ackerson, S.M., Romney, C., Schuck, P.L., and Stewart, J.A. (2021). To Join or Not to Join: Decision Points Along the Pathway to Double-Strand Break Repair vs. Chromosome End Protection. Front. Cell Dev. Biol. *9*, 708763.

34. Park, J., Long, D.T., Lee, K.Y., Abbas, T., Shibata, E., Negishi, M., Luo, Y., Schimenti, J.C., Gambus, A., Walter, J.C., and Dutta, A. (2013). The MCM8-MCM9 complex promotes RAD51 recruitment at DNA damage sites to facilitate homologous recombination. Mol. Cell Biol. *33*, 1632–1644.

35. Lee, K.Y., Im, J.S., Shibata, E., Park, J., Handa, N., Kowalczykowski, S.C., and Dutta, A. (2015). MCM8-9 complex promotes resection of double-strand break ends by MRE11-RAD50-NBS1 complex. Nat. Commun. *6*, 7744.

36. Nimonkar, A.V., Genschel, J., Kinoshita, E., Polaczek, P., Campbell, J.L., Wyman, C., Modrich, P., and Kowalczykowski, S.C. (2011). BLM-DNA2-RPA-MRN and EXO1-BLM-RPA-MRN constitute two DNA end resection machineries for human DNA break repair. Genes Dev. *25*, 350–362.

37. Sajish, M., and Schimmel, P. (2015). A human tRNA synthetase is a potent PARP1-activating effector target for resveratrol. Nature *519*, 370–373.

38. Formosa, T., and Winston, F. (2020). The role of FACT in managing chromatin: disruption, assembly, or repair? Nucleic Acids Res. *48*, 11929–11941.

39. Miyamoto, Y., Kitamura, N., Nakamura, Y., Futamura, M., Miyamoto, T., Yoshida, M., Ono, M., Ichinose, S., and Arakawa, H. (2011). Possible existence of lysosome-like organella within mitochondria and its role in mitochondrial quality control. PLoS One *6*, e16054.

40. Schumacher, B., Pothof, J., Vijg, J., and Hoeijmakers, J.H.J. (2021). The central role of DNA damage in the ageing process. Nature *592*, 695–703.

41. Curtin, N.J. (2012). DNA repair dysregulation from cancer driver to therapeutic target. Nat. Rev. Cancer *12*, 801–817.

42. Xu, Z., Zan, H., Pone, E.J., Mai, T., and Casali, P. (2012). Immunoglobulin class-switch DNA recombination: induction, targeting and beyond. Nat. Rev. Immunol. *12*, 517–531.

43. Nemazee, D. (2006). Receptor editing in lymphocyte development and central tolerance. Nat. Rev. Immunol. *6*, 728–740.

44. Papavasiliou, F.N., and Schatz, D.G. (2002). Somatic hypermutation of immunoglobulin genes: merging mechanisms for genetic diversity. Cell *109*, S35–S44.

45. Schatz, D.G., and Ji, Y. (2011). Recombination centres and the orchestration of V(D)J recombination. Nat. Rev. Immunol. *11*, 251–263.

46. Mombaerts, P., Iacomini, J., Johnson, R.S., Herrup, K., Tonegawa, S., and Papaioannou, V.E. (1992). RAG-1-deficient mice have no mature B and T lymphocytes. Cell *68*, 869–877.

47. Shinkai, Y., Rathbun, G., Lam, K.P., Oltz, E.M., Stewart, V., Mendelsohn, M., Charron, J., Datta, M., Young, F., Stall, A.M., et al. (1992). RAG-2-deficient mice lack mature lymphocytes owing to inability to initiate V(D)J rearrangement. Cell *68*, 855–867.

48. Cascalho, M., Wong, J., Steinberg, C., and Wabl, M. (1998). Mismatch repair co-opted by hypermutation. Science *279*, 1207–1210.

49. Vora, K.A., Tumas-Brundage, K.M., Lentz, V.M., Cranston, A., Fishel, R., and Manser, T. (1999). Severe attenuation of the B cell immune response in Msh2-deficient mice. J. Exp. Med. *189*, 471–482.

50. Danilova, N., Bussmann, J., Jekosch, K., and Steiner, L.A. (2005). The immunoglobulin heavy-chain locus in zebrafish: identification and expression of a previously unknown isotype, immunoglobulin Z. Nat. Immunol. *6*, 295–302.

51. Busch, D.H., and Pamer, E.G. (1999). T cell affinity maturation by selective expansion during infection. J. Exp. Med. *189*, 701–710.

52. Slifka, M.K., and Whitton, J.L. (2001). Functional avidity maturation of CD8(+) T cells without selection of higher affinity TCR. Nat. Immunol. *2*, 711–717.

53. DeGrendele, H.C., Kosfiszer, M., Estess, P., and Siegelman, M.H. (1997). CD44 activation and associated primary adhesion is inducible via T cell receptor stimulation. J. Immunol. *159*, 2549–2553.

54. Baaten, B.J.G., Tinoco, R., Chen, A.T., and Bradley, L.M. (2012). Regulation of Antigen-Experienced T Cells: Lessons from the Quintessential Memory Marker CD44. Front. Immunol. *3*, 23.

55. Kaur, J., and Debnath, J. (2015). Autophagy at the crossroads of catabolism and anabolism. Nat. Rev. Mol. Cell Biol. *16*, 461–472.

56. Hewitt, G., and Korolchuk, V.I. (2017). Repair, Reuse, Recycle: The Expanding Role of Autophagy in Genome Maintenance. Trends Cell Biol. *27*, 340–351.

57. Gomes, L.R., Menck, C.F.M., and Leandro, G.S. (2017). Autophagy Roles in the Modulation of DNA Repair Pathways. Int. J. Mol. Sci. *18*, 2351.

58. SenGupta, T., Torgersen, M.L., Kassahun, H., Vellai, T., Simonsen, A., and Nilsen, H. (2013). Base excision repair AP endonucleases and mismatch repair act together to induce checkpoint-mediated autophagy. Nat. Commun. *4*, 2674.

59. Dan, X., Babbar, M., Moore, A., Wechter, N., Tian, J., Mohanty, J.G., Croteau, D.L., and Bohr, V.A. (2020). DNA damage invokes mitophagy through a pathway involving Spata18. Nucleic Acids Res. *48*, 6611–6623.

60. Aman, Y., Schmauck-Medina, T., Hansen, M., Morimoto, R.I., Simon, A.K., Bjedov, I., Palikaras, K., Simonsen, A., Johansen, T., Tavernarakis, N., et al. (2021). Autophagy in healthy aging and disease. Nat. Aging *1*, 634–650.

61. Chang, C., Jensen, L.E., and Hurley, J.H. (2021). Autophagosome biogenesis comes out of the black box. Nat. Cell Biol. *23*, 450–456.

62. Gutierrez, M.G., Master, S.S., Singh, S.B., Taylor, G.A., Colombo, M.I., and Deretic, V. (2004). Autophagy is a defense mechanism inhibiting BCG and Mycobacterium tuberculosis survival in infected macrophages. Cell *119*, 753–766.

63. Golovkine, G.R., Roberts, A.W., Morrison, H.M., Rivera-Lugo, R., McCall, R.M., Nilsson, H., Garelis, N.E., Repasy, T., Cronce, M., Budzik, J., et al. (2023). Autophagy restricts Mycobacterium tuberculosis during acute infection in mice. Nat. Microbiol. *8*, 819–832.

64. Wang, F., Peters, R., Jia, J., Mudd, M., Salemi, M., Allers, L., Javed, R., Duque, T.L.A., Paddar, M.A., Trosdal, E.S., et al. (2023). ATG5 provides host protection acting as a switch in the atg8ylation cascade between autophagy and secretion. Dev. Cell *58*, 866–884.e8.

65. Koster, S., Upadhyay, S., Chandra, P., Papavinasasundaram, K., Yang, G., Hassan, A., Grigsby, S.J., Mittal, E., Park, H.S., Jones, V., et al. (2017). Mycobacterium tuberculosis is protected from NADPH oxidase and LC3-associated phagocytosis by the LCP protein CpsA. Proc. Natl. Acad. Sci. USA *114*, E8711–E8720.

66. Aylan, B., Bernard, E.M., Pellegrino, E., Botella, L., Fearns, A., Athanasiadi, N., Bussi, C., Santucci, P., and Gutierrez, M.G. (2023). ATG7 and ATG14 restrict cytosolic and phagosomal Mycobacterium tuberculosis replication in human macrophages. Nat. Microbiol. *8*, 803–818.

67. Strong, E.J., and Lee, S. (2020). Targeting Autophagy as a Strategy for Developing New Vaccines and Host-Directed Therapeutics Against Mycobacteria. Front. Microbiol. *11*, 614313.

68. Ponpuak, M., Davis, A.S., Roberts, E.A., Delgado, M.A., Dinkins, C., Zhao, Z., Virgin, H.W., 4th, Kyei, G.B., Johansen, T., Vergne, I., and Deretic, V. (2010). Delivery of cytosolic components by autophagic adaptor protein p62 endows autophagosomes with unique antimicrobial properties. Immunity *32*, 329–341.

69. Seto, S., Tsujimura, K., Horii, T., and Koide, Y. (2013). Autophagy adaptor protein p62/SQSTM1 and autophagy-related gene Atg5 mediate autophagosome formation

in response to Mycobacterium tuberculosis infection in dendritic cells. PLoS One *8*, e86017.

70. Zhang, R., Varela, M., Vallentgoed, W., Forn-Cuni, G., van der Vaart, M., and Meijer, A.H. (2019). The selective autophagy receptors Optineurin and p62 are both required for zebrafish host resistance to mycobacterial infection. PLoS Pathog. *15*, e1007329.
71. Neefjes, J., Jongsma, M.L.M., Paul, P., and Bakke, O. (2011). Towards a systems understanding of MHC class I and MHC class II antigen presentation. Nat. Rev. Immunol. *11*, 823–836.
72. Kirkin, V., McEwan, D.G., Novak, I., and Dikic, I. (2009). A role for ubiquitin in selective autophagy. Mol. Cell *34*, 259–269.
73. Shaid, S., Brandts, C.H., Serve, H., and Dikic, I. (2013). Ubiquitination and selective autophagy. Cell Death Differ. *20*, 21–30.
74. Jena, K.K., Kolapalli, S.P., Mehto, S., Nath, P., Das, B., Sahoo, P.K., Ahad, A., Syed, G.H., Raghav, S.K., Senapati, S., et al. (2018). TRIM16 controls assembly and degradation of protein aggregates by modulating the p62-NRF2 axis and autophagy. EMBO J. *37*, e98358.
75. Jongsma, M.L.M., Berlin, I., Wijdeven, R.H.M., Janssen, L., Janssen, G.M.C., Garstka, M.A., Janssen, H., Mensink, M., van Veelen, P.A., Spaapen, R.M., and Neefjes, J. (2016). An ER-Associated Pathway Defines Endosomal Architecture for Controlled Cargo Transport. Cell *166*, 152–166.
76. Odegard, V.H., and Schatz, D.G. (2006). Targeting of somatic hypermutation. Nat. Rev. Immunol. *6*, 573–583.
77. Abuetabh, Y., Wu, H.H., Chai, C., Al Yousef, H., Persad, S., Sergi, C.M., and Leng, R. (2022). DNA damage response revisited: the p53 family and its regulators provide endless cancer therapy opportunities. Exp. Mol. Med. *54*, 1658–1669.
78. Chen, Q., Sun, L., and Chen, Z.J. (2016). Regulation and function of the cGAS-STING pathway of cytosolic DNA sensing. Nat. Immunol. *17*, 1142–1149.
79. Bredemeyer, A.L., Helmink, B.A., Innes, C.L., Calderon, B., McGinnis, L.M., Mahowald, G.K., Gapud, E.J., Walker, L.M., Collins, J.B., Weaver, B.K., et al. (2008). DNA double-strand breaks activate a multi-functional genetic program in developing lymphocytes. Nature *456*, 819–823.
80. Bednarski, J.J., and Sleckman, B.P. (2019). At the intersection of DNA damage and immune responses. Nat. Rev. Immunol. *19*, 231–242.
81. Yang, R., Deng, Y., Huang, B., Huang, L., Lin, A., Li, Y., Wang, W., Liu, J., Lu, S., Zhan, Z., et al. (2021). A core-shell structured COVID-19 mRNA vaccine with favorable biodistribution pattern and promising immunity. Signal Transduct. Targeted Ther. *6*, 213.
82. Wang, T., Yan, B., Lou, L., Lin, X., Yu, T., Wu, S., Lu, Q., Liu, W., Huang, Z., Zhang, M., et al. (2019). Nlrc3-like is required for microglia maintenance in zebrafish. J. Genet. Genom. *46*, 291–299.
83. Xiang, Z.-H., Sun, R.-F., Lin, C., Chen, F.-Z., Mai, J.-T., Liu, Y.-X., Xu, Z.-Y., Zhang, L., and Liu, J. (2017). Immunogenicity and Protective Efficacy of a Fusion Protein Tuberculosis Vaccine Combining Five Esx Family Proteins. Front. Cell. Infect. Microbiol. *7*, 226.